# The Primary Pattern Generator Part II–Mechanical Design

By G. J. W. KOSSYK, J. P. LAICO, L. RONGVED and J. W. STAFFORD

(Manuscript received July 10, 1970)

## I. INTRODUCTION

The primary pattern generator (PPG) is an electromechanical light-scanning system with an unusual combination of speed and accuracy. A 10-$\mu$m-diameter light spot can be addressed successively to any or all points of a 26,000-wide by 32,000-long rectangular point array with 7-$\mu$m vertical and horizontal spacing in about ten minutes. This corresponds to a scanning rate of one spot per 600 nanoseconds. The light spot is placed repeatedly to an accuracy of about a $\pm$7-$\mu$m total accumulated error over the whole array, and the vertical and horizontal spacing between points is maintained within $\pm$1 $\mu$m.

The rectangular point array is scanned one line at a time at the rate of 53 lines per second by successive sweeps of a monitored laser beam across the width of the array interposed by 7-$\mu$m steps of the photographic plate in the perpendicular direction. The essential components of the scanning system are shown in Fig. 1. The laser generates a light beam which, by various stationary mirrors, is directed to the acoustooptic modulator. When this modulator is turned on, a small portion of the laser beam is slightly deflected and is denoted the write beam. The major portion of the light beam, called here the code beam, passes through the modulator with no directional change. When the modulator is turned off, the light beam passes through unchanged. The response time of the modulator is of the order of 10 nanoseconds which is very small compared to the 600-nanosecond period it takes the scanning beam to move from one addressable point to the next.

By further fixed mirrors and lenses, the code and write beam is brought to focus at neighboring points near the edge of the photographic plate.

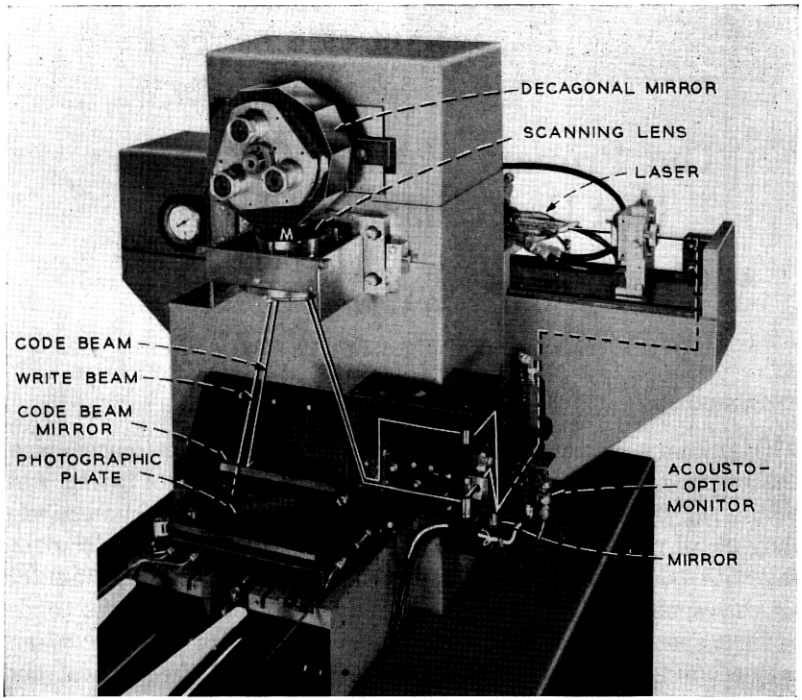


Fig. 1—Primary pattern generator.

By means of the scanning lens and the decagonal mirror, the focused spot of the write beam is imaged onto the photographic plate. The focused point of the code beam is, by the same means and one additional code beam mirror, imaged onto a code plate. The code beam is intercepted by the code plate except at 7.0-$\mu$m-wide transparent lines on 14-$\mu$m centers. The light passing through these transparent lines is collected in a photocell by means of a Fresnel lens. As the decagonal mirror turns, the two beams move together. The code beam, by pulsing the photodetector, yields positional information to the computer which, by means of the modulator, regulates the write beam on or off as required for proper exposure of the photographic plate.

The decagonal mirror spins at 300 rpm resulting in 53 write-beam sweeps per second. The 10 facets of the decagonal mirror are inclined to the mirror's radial symmetry axis at a very small angle which is identical for all facets within $\pm\frac{1}{4}$ of one second of arc. Furthermore, the mirror's radial-symmetry axis spins with a wobble less than 1/10

of one second of arc. Therefore, any sweep of the write beam when the photographic plate is fixed traces lines that are separated by no more than $\pm\frac{1}{2}$ $\mu$m.

The 300-rpm speed of the decagonal mirror results in about 11-ms-duration sweeps across the photographic plate, with about a 7-ms-long period between the end of one and the beginning of the next sweep. The computer may write in every sweep, and the step system must be designed so that a step may be completed in the 7-ms period between sweeps. If the computer writes in every sweep, the table steps at 53 steps per second. If the computer cannot write in every sweep, one or more steps are skipped as required for the computer to catch up. This step motion is a sophisticated vibration-free one where each step is equal to the next within $\pm\frac{1}{2}$ $\mu$m, and the total accumulative error over 32,000 steps is about $\pm 5$ $\mu$m assuming temperature control within 0.2°C.

## II. MATERIALS SELECTION

The material used for the major PPG structure is Meehanite GC40. This material was chosen for its great dimensional stability with time. To insure that the material was initially stress-free, a three-step heat treatment-machining sequence was used. Briefly:

(*i*) After casting
- (*a*) Heat to 1600°F. Hold 2 hours.
- (*b*) Cool to 1250°F at 35°F per hour.
- (*c*) Hold at 1250°F for 10 hours.
- (*d*) Cool to 200°F at 20-25°F per hour.

(*ii*) After Rough Machining (allow 0.020″ for final machining)
Thermally cycle: 210°F to 400°F to −120°F to 400°F to 200°F. Hold at −120°F and 400°F for 2 hours.
Final cooling to 200°F must not exceed 25°F per hour.

(*iii*) After Dual Machining
- (*a*) Heat to 300°F. Hold for 6 hours.
- (*b*) Cool to 200°F at 20-25°F per hour.

The residual stress after heat treatment will not exceed 200 psi, resulting in a maximum relaxation strain of about 10 microinches per inch. Micro-creep tests conducted at Battelle Institute indicated that most of this relaxation occurs in the first four to six weeks which is before assembly of the pattern generator. Thus, only a few microinches per inch is expected during the life of the pattern generator.

## III. TWO SPECIAL AXIAL ALIGNMENTS

Two very accurate axial alignments are made in the pattern generator. In one, the axis of an air bearing is aligned with the radial-symmetry axis of the decagonal mirror. In the other, the axis of the air bearing is aligned with the direction of motion of the step table. Both alignments use an elastic micromanipulator which was developed especially for the pattern generator. The alignments are essentially identical and only the decagonal mirror alignment is described here.

### 3.1 *The Elastic Micromanipulator*

The elastic micromanipulator is based upon a very elementary mechanical deamplification device. It consists of two springs that are connected in series and deflected against a support. In the static case, the total deflection of the spring, $\Delta\delta_1$, is related to the deflection of the interface of the springs, $\Delta\delta_2$, by the relationship

$$\Delta\delta_2 = \frac{k_1}{k_1 + k_2} = \Delta\delta_2$$

where $k_1$ and $k_2$ are the respective spring constants. The motion, $\Delta\delta_1$, is thus directly related to $\Delta\delta_2$ by the deamplification factor $F = k_1/(k_1 + k_2)$, which can be made as small as one pleases by choosing $k_2 \gg k_1$. In order to use such a device as a micromanipulator, one provides a fine screw to manually produce the deflection, $\Delta\delta_1$, and one attaches the body to be moved to the spring interface so that the corresponding body motion is $\Delta\delta_2$ as shown in the lower part of Fig. 2.

### 3.2 *Alignment of the Decagonal Mirror*

The adjustment for axial alignment of the decagonal mirror consists of three elastic micromanipulators placed 120° apart and equidistant from the symmetry axis. Between the face of the air-bearing spindle and one side of the mirror are the three stiff springs and, on the other side of the mirror directly opposite to these stiff springs, are the three soft springs which can be pressed against the mirror individually by three fine-adjusting screws.

The nature of the three stiff springs requires some explanation. The air-bearing face is machined with three raised $\frac{1}{4}'' \times \frac{1}{4}''$ areas as indicated in Fig. 3. The surface of these areas is finished machined with a stationary tool when the air bearing is spinning so that their surfaces lie in a plane normal to the air-bearing axis within about a second of arc. The decagonal mirror has an optically flat end face and this face

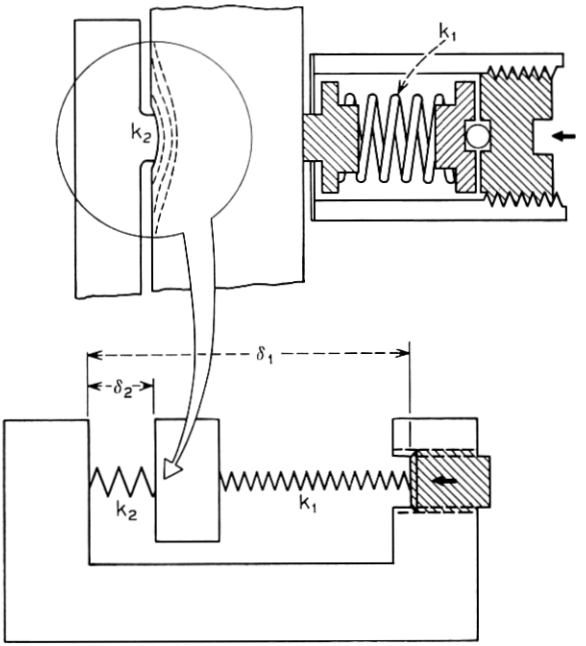


Fig. 2—Elastic micromanipulator.

is placed directly against these three pads. As the mirror is pressed against these raised areas by the soft springs on the opposite side of the mirror, the pads elastically indent the mirror as indicated on the upper part of Fig. 2. There is also some corresponding local indentation of the air-bearing face. Except for these small local regions of deformation, the mirror and the air bearing remain essentially rigid and the elastic deformation in the three small regions serves the purpose of the three stiff springs. The various mechanical elements are shown in detail in Fig. 4.

The relationship between the force exerted by the soft springs and the corresponding deflection of the stiff springs can be worked out from a classical elasticity solution due to J. Boussinesq. From this solution one can determine the effective spring constant associated with each of the three stiff springs. They are given approximately by

$$k_2 = 2 \cdot 10^6 \text{ lb/in.}$$

The soft springs on the opposite side have a spring constant given by

$$k_1 = 6 \cdot 10^2 \text{ lb/in}$$

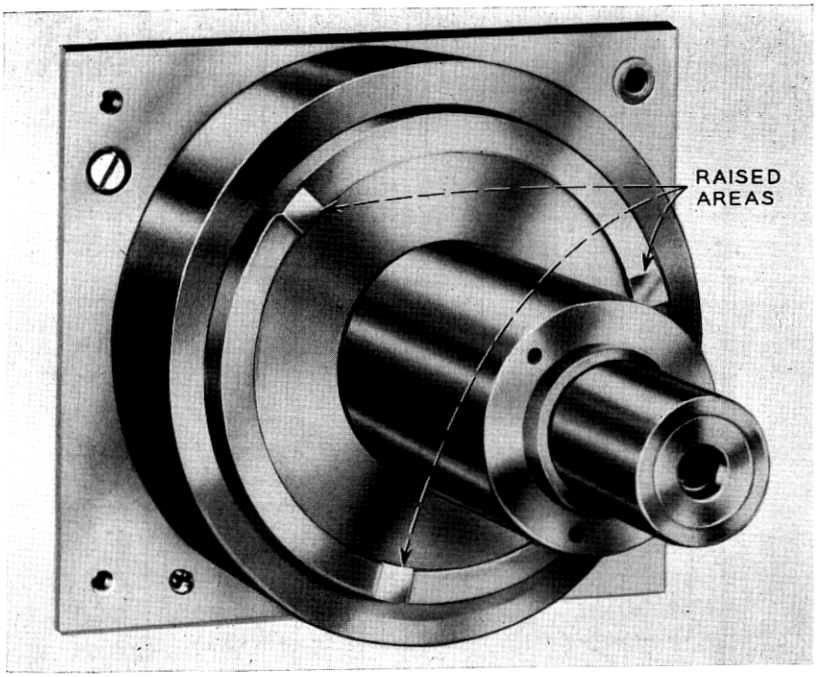


Fig. 3—Air-bearing spindle with raised areas.

and the amplification factor, $F$, works out to be about

$$F = 3 \cdot 10^{-4}.$$

The pitch of the adjusting screws is 40 turns per inch, and thus for one complete revolution of the adjusting screws the mirror will move about $18 \cdot 10^{-2}$ microns. When only one adjusting nut is advanced, the mirror will rotate about an axis passing through the two raised areas opposite the other two adjusting nuts. The raised areas are separated by about 7 cm, and thus the resulting rotation of the mirror equals about (0.6) second of arc per revolution of the adjusting nut. Since the adjustment is carried out together with an instrument to measure the mirror axis run out, there is no need to know this relationship exactly.

In the PPG, the mirror axis is aligned with the air-bearing axis to $\frac{1}{10}$ of a second, and we know that the adjustment remains stable to this accuracy over long periods.

When the mirror facets are measured to perform the final grinding operations, the mirror is aligned to $\frac{1}{50}$ of a second. This more precise

adjustment has been demonstrated to be stable over several days, but it has not been evaluated on a long-term basis.

## IV. THE STEPPING SYSTEM

There are two simple and fundamental concepts involved in the pattern-generator stepping system. One of these is a special electronic drive for the step motor used in the mechanical drive of the stepping system. The other is tuning of the natural frequency of the second mode of motion of the mechanical drive. Together these two concepts permit vibration-free stepping in the absence of passive damping. There are also several practical problems involved in the construction of the step table. One describes here first the two simple concepts, next the problems of construction, and last some experimental results.

### 4.1 *The Special Electronic Drive*

In order to describe the special electronic drive, first one describes certain characteristics of the stepping motor. The motor torque, $T$, as a function of the angular position of the armature, $\theta$, is shown in Fig. 5a for a given current in the two motor windings. The amplitude of the sinusoidally varying torque is called the holding torque. The hold-

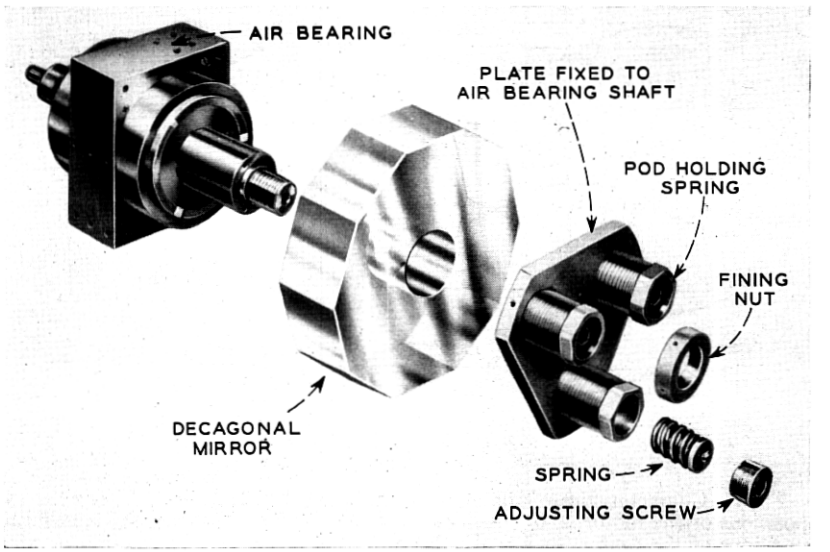


Fig. 4—Telescopic view of the decagonal mirror adjustment.

ing torque is proportional to the current in the motor windings. The magnitude of this current is usually kept constant, and only its direction is changed in the normal operation of the stepping motor. The effect of successively changing the direction of the current in each motor winding is indicated in Fig. 5b.

The mechanics of a simple operation of a stepping motor are essentially as follows: Assume the motor to be at rest in step position, $n$, which is one of the stable-equilibrium positions associated with the motor torque indicated by the solid curve in Fig. 6. Let the current be changed in one winding, thus bringing about the motor torque indicated by the dotted curve. The motor will now accelerate towards the step position $n + 1$ and, depending upon the damping in the motor, assumed less than critical, it will vibrate about the new position with decaying amplitude. This vibration is completely intolerable for the present application. Furthermore, if the motor is stepped continuously, vibration build-up from one step to the other occurs. To eliminate the vibration, the motor is provided with a special electronic drive. This drive provides three timed current settings for the motor per step which are applied as follows: Assume as before that the motor is at rest in position $n$ as indicated in Fig. 6. The current is now reversed

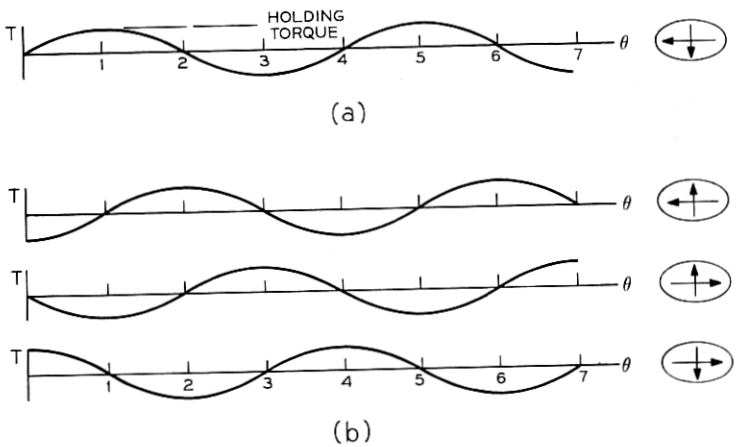


Fig. 5—Characteristics of the stepping motor. (a) 0, 1, 2, $\cdots$, $N$, are the step positions of the motor. 2, 6, $\cdots$, $(2 + 4I)$, where $I$ is an integer, are equilibrium positions of the motor for a particular current direction in the two-motor windings as schematically indicated by the arrows in the ellipse on the right. (b) The motor torque as a function of theta is simply translated by one step each time the current is reversed in one winding.

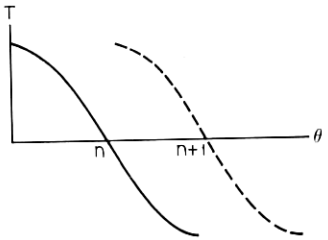


Fig. 6—Motor torque, $T$, as a function of angular position, $\theta$.

in one winding for a timed period, $t_1$, bringing about the motor torque indicated by the dotted curve. As before, this will accelerate the motor towards its new step position, $n + 1$. However, $t_1$ is adjusted such that at the end of this timed period the motor is at a point about half way between $n$ and $n + 1$, and it is of course still moving. The current is now reversed again in the same winding for another time period, $t_2$, bringing about the torque indicated by the solid curve in Fig. 6. This torque decelerates the step motor until it stops, and $t_1$ and $t_2$ are timed such that the point at which the motor stops coincides with the new step position, $n + 1$. The current in the same winding is now reversed a third time, producing the motor torque indicated by the dotted curve. This third current setting will hold the motor in the new equilibrium position until one wishes to make another step. This stepping technique produces vibration-free stepping without passive damping. Such an electronic device has been used previously in Bell Laboratories for a magnetic tape drive.

### 4.2 *A Tuned Two-Degrees-of-Freedom System*

In the previous description of the special motor drive it was tacitly assumed that the stepping motor and all that it drives behaves as a single-degree-of-freedom system, i.e., that the motion of all bodies involved can be determined from a single independent variable. This state exists if such things as backlash, elastic deformation of parts, etc., are negligible. If the time to complete a single step is made sufficiently long, say by decreasing the motor torque, our step system will behave sensibly as a single-degree-of-freedom mechanical system involving only rigid-body motion. However, if the time to complete a step is made short enough as was the case in the pattern generator, one will also excite noticeable motion involving elastic deformation in components of the system. One is then confronted with a much more

complicated multidegree-of-freedom mechanical system. Specifically, there was one deformational mode of motion that could not be eliminated. The special motor drive does not then by itself yield vibration-free stepping. One describes here how we were able to control this deformational mode by tuning its natural frequency.

The stepping table is shown in Fig. 7. It consists of a stepping motor driving the shaft of a ball-lead screw, a thrust bearing preventing axial motion of the shaft relative to the rigid base, a step table on linear roller bearing ways and driven by the nut of the lead screw. There are two modes of motion that come into play in this stepping system: (*i*) The motion in which all bodies remain rigid and involving shaft rotation and linear table motion as constrained by the lead-screw pitch. One denotes this mode the ideal rigid-body mode. (*ii*) The mode of motion where the table, as in the first mode, moves as a rigid body on

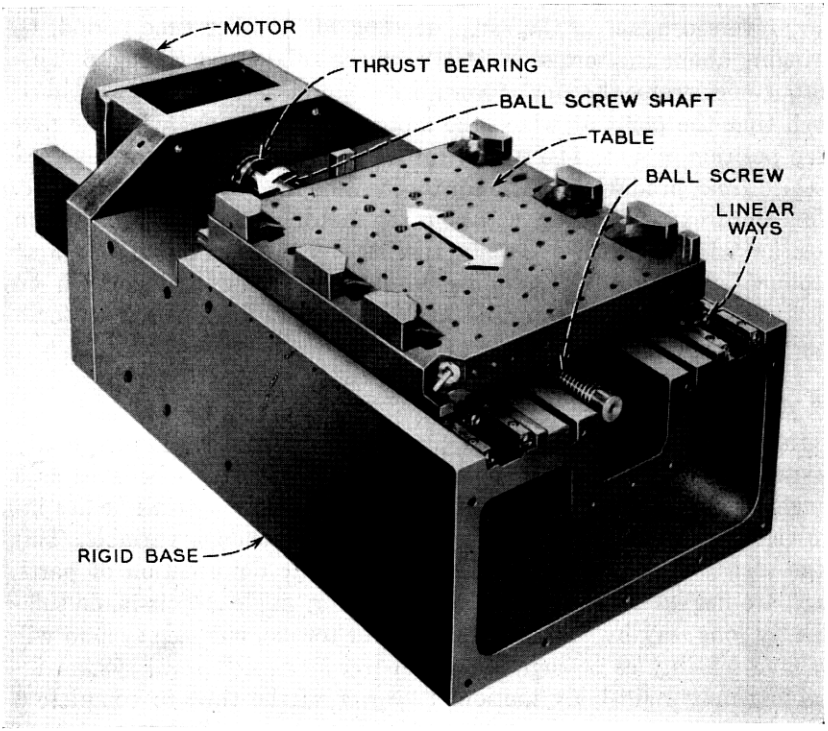


Fig. 7—Stepping system.

its ways but now as a result of elastic deformation primarily of the Hertz type that occurs in the balls and races of the lead screw.

A simple analysis of this two-degrees-of-freedom system reveals an interesting characteristic, namely, that by an adjustment of the natural frequency of the second mode of motion, the special electronic motor drive will step the table with no vibration in either mode. Subsequent experiments proved that such mechanical tuning is a practical matter. In order to describe the essential mechanics involved, some aspects of the simple analysis are given here.

Because of special mechanical characteristics of the step table the two modes of motion mentioned above, namely, the ideal rigid-body mode and the mode involving deformation in the ball screw, are very nearly the normal modes of the system. Therefore, the shaft rotation under the action of the motor torque is sensibly unaffected by the elastic deformation in the ball screw and can be calculated quite accurately, taking only the rigid-body mode into account. The second mode of motion can be equally accurately calculated, taking it to be a single-degree-of-fredom system whose support is given an inexorable motion identical to the table motion associated with the rigid-body mode. The equations for this determination of the first and second mode are

$$T = I\ddot{\theta},$$

$$x_0 = \frac{p}{2\pi}\theta,$$

$$\ddot{x} + \ddot{x}_0 = -\omega^2 x,$$

where $T$ is the motor torque, $I$ is the sum of the rotatory inertia of the motor and lead-screw shaft plus an equivalent table rotatory inertia, $\theta$ is the angular position of the motor, $x_0$ is the first-mode table motion, $x$ is the second-mode table motion, $p$ is the lead-screw pitch, $\omega$ is the circular natural frequency of the second mode, and dots indicate time derivatives. One assumes now first that the motor torque is a constant over the acceleration period $t_1$ and the same constant with negative sign during the deceleration period $t_2$ . Secondly, one assumes $t_1 = t_2$ and that the constant torque is selected so that $\dot{x}_0$ is zero when $x_0$ is increased by one step, i.e., the special drive is adjusted to give no vibration in $x_0$ at the end of a step. Lastly, one assumes that $x$ and $\dot{x}$ are zero at the beginning of a step. One obtains then for the amplitude of vibration

in the second mode, $A$,

$$A = \bar{x}_0 \frac{\sin^2 (\pi f \bar{t}/2)}{(\pi f \bar{t}/2)^2}$$

where $\bar{x}_0$ is the length of one step, $f = \omega/2\pi$, and $\bar{t} = t_1 + t_2$. One notes now that $A = 0$ when $f\bar{t}/2$ is an integer. According to this simple analysis, there should be no vibration if $f = 286$ cps when $\bar{t} = 7 \cdot 10^{-3}$ s as required in the pattern generator. This frequency corresponds closely to the frequency determined both experimentally and from a more rigorous numerical analysis at which vibration was found to vanish. The vibration amplitude, $A$, is plotted in Fig. 8 as a function of $f$. This curve reveals another important point, namely, that where $A$ is zero, the slope of the curve is also zero. For that reason, there is no need to adjust the frequency of the second mode accurately to effectively eliminate vibration, which would have been impractical. One notes that the above solution applies to continuous stepping only when $f\bar{t}/2$ is an integer since only then are $x$ and $\dot{x}$ zero at the beginning of each step. If vibration in $x$ occurs, one has to contend with vibration build-ups from one step to the next.

The rigid-body mode, $f = \infty$, is plotted together with the actual table motion in Fig. 9. The difference between these curves is essentially due to motion in the second mode. One notes that the second mode, as the first, is excited only during the times $t_1$ and $t_2$, and no subsequent motion occurs until the table is stepped again.

### 4.3 *Some Practical Problems of Construction*

Several problems were encountered in the construction of the step table to make it, in fact, behave as the two-degrees-of-freedom system analyzed. A major problem was to reduce the number of degrees of freedom of the system to two. This was done by increasing the natural frequency of the various other modes to a point where the step motion would not noticeably excite them. Our effort in this respect is reflected in the very massive and stiff structure of the pattern generator.

Of particular interest also is the very massive support for the thrust bearing, noticeable in Fig. 7. A particular thrust bearing was selected which enabled us to get rid of a very objectionable third mode of motion in which the ball-screw shaft would move axially by elastically deforming the thrust bearing and its support. A very difficult problem was to find lead screws with a combination of high stiffness of the nuts axial deformation relative to the shaft and low-frictional torque. We found ball-lead screws to be far superior in this respect to lead screws with acme threads.

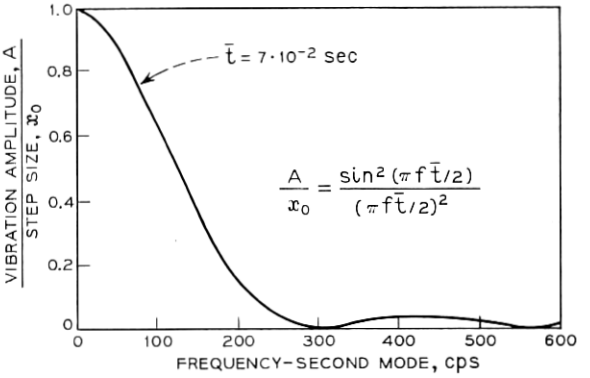


Fig. 8—Vibration amplitude, $A$, of the second mode as a function of its frequency for a fixed step time, $\bar{t} = 7$ ms.

### 4.4 *Lead Screw Life Tests*

One of the most critical mechanical requirements of the PPG is that the drive train of the system have a sufficiently long life so that many years of product can be made without changing essential items which would affect the reproducibility accuracy of the system. One sees from Fig. 8 that a drive train-table combination whose stiffness yields a frequency of about 280 cps is desirable. To insure step accu-

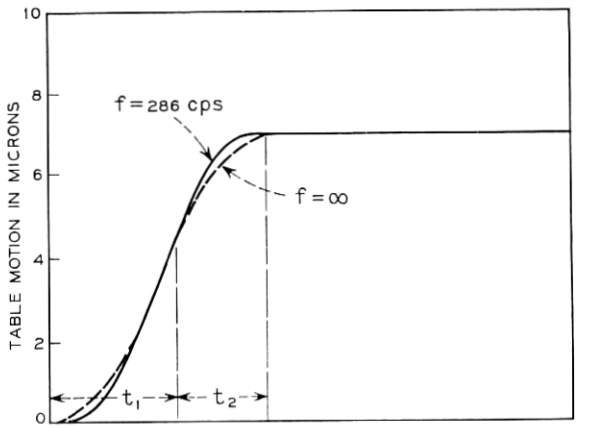


Fig. 9—Ideal rigid-body mode, $f = \infty$, superimposed on the actual table motion, $f = 286$ cps. The discrepancy between the two curves is very nearly the motion of the second mode. One notes that both modes are excited during $t_1$ and $t_2$, but no motion persists in either mode once a step is completed.

racy, it was desired that the stepping-system stiffness be great enough to yield a frequency of 280 cps and the frictional torque should be considerably lower than the stepping-motor holding torque so as to minimize step error due to friction. A preload of 25 pounds on the ball screw was found to yield the desired system stiffness and torque to break static friction.

The test setup used to establish the life test of the mechanical components of the drive train is shown in Fig. 10. The life-test setup duplicates the essential features of the PPG drive train.

The status of the life-test equipment was monitored by periodically checking the torque to break static friction and the stiffness of each system. The stiffness was measured by determining the rigid-body resonant frequency of the drive train-table combination and then calculating the stiffness. The stiffness was also checked occasionally by statically measuring the drive-train stiffness by applying a known load and measuring the table deflection relative to the thrust-bearing support.

One sees from Fig. 11, which is typical of the data taken, that there has been a pattern of decreasing torque-to-break static friction. Similarly, from Fig. 12, the stiffness measurements for the units have shown a tendency to increase with time.

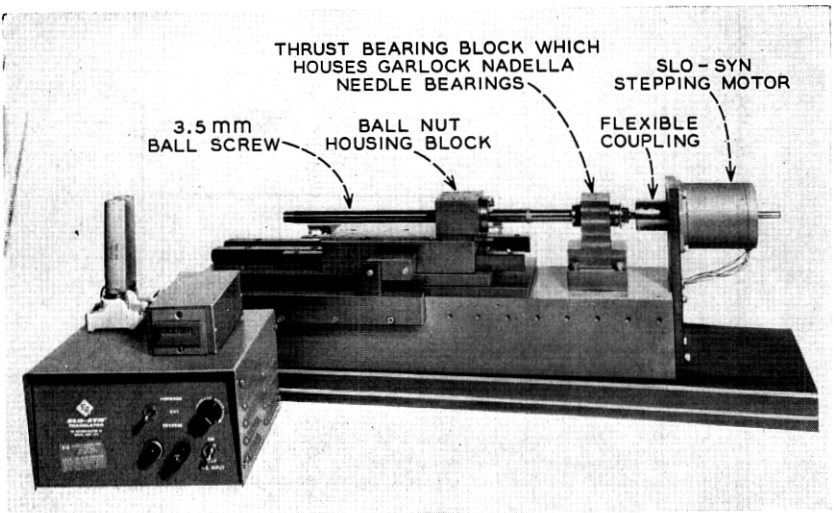


Fig. 10—Typical life-test setup.

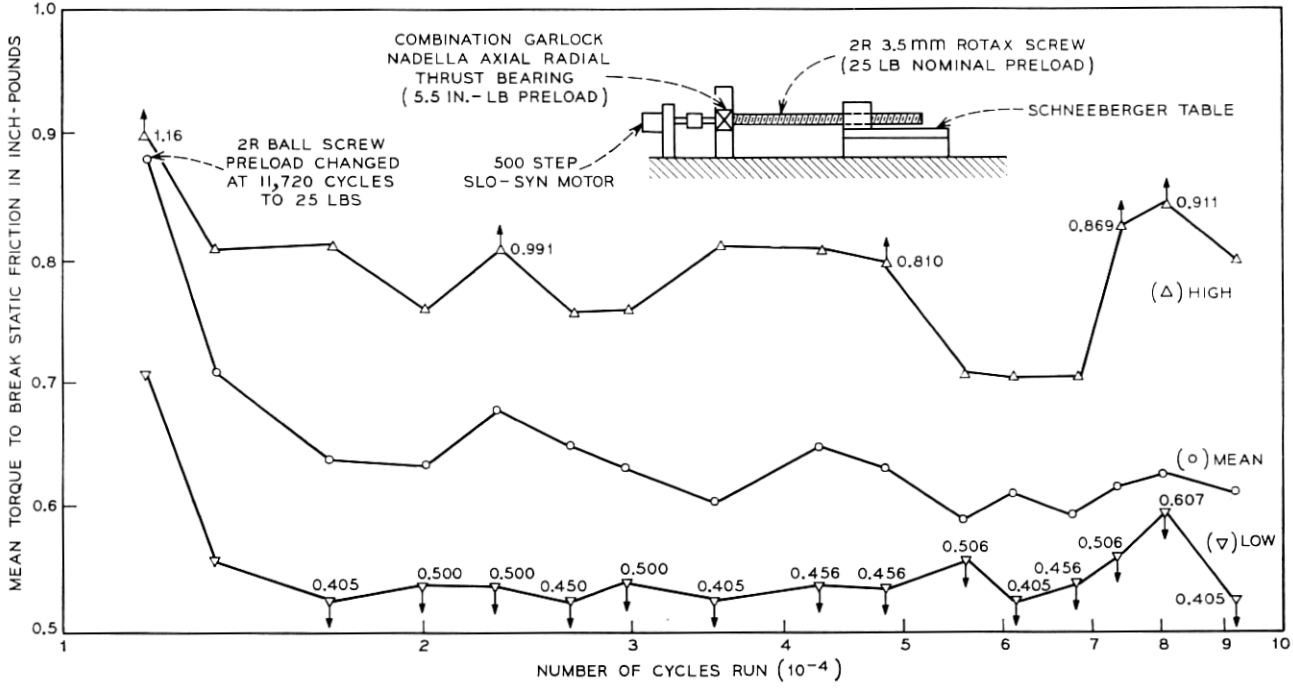


Fig. 11—Mean torque-to-break static friction versus cycles run on 2R life-test setup. Note: 1. Distance traveled per cycle = 19″; 2. Time per cycle = 190 s.

During the life test, a decrease in torque and an increase in stiffness can be attributed to the fact that the screw and bearings are being burnished (i.e., worn in) and hence, the riding surfaces are more uniform and smoother. Furthermore, as things become smoother, more balls of the ball screw and needles of the thrust bearing become fully effective.

### 4.5 *Stepping Test Measurements*

The accuracy of the step table as determined experimentally is briefly as follows: Steps are reproducible to $\pm\frac{1}{4}$ $\mu$m. This reproducibility accuracy is primarily the result of some unavoidable coulomb friction in the drive and a small amount of vibration about the equilibrium position. The absolute accuracy of steps is such that all steps are equal within $\pm\frac{1}{2}$ $\mu$m.

Experimental determination of the table motion as a function of time is given in Fig. 13.

Straightness of table travel with minimal transverse and rotary motions is necessary to achieve reproducibility of spot positions on the photographic plate. A table mounted on preloaded roller bearings was employed to achieve the required accuracy. Measurements showed that

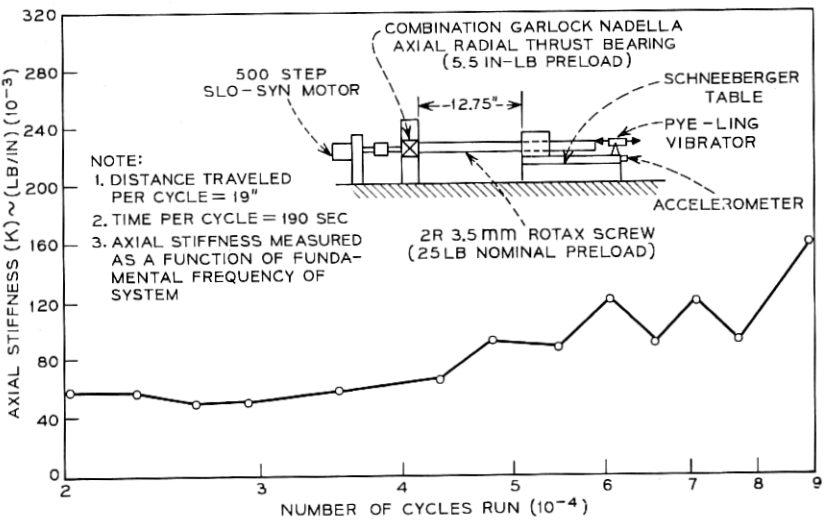


Fig. 12—Axial stiffness of 2R life-test setup versus cycles run. Note: 1. Distance traveled per cycle = 19"; 2. Time per cycle = 190 s; 3. Axial stiffness measured as a function of fundamental frequency of system; 4. Axial stiffness measured directly, using a federal gage to measure table deflection ($\Delta$).

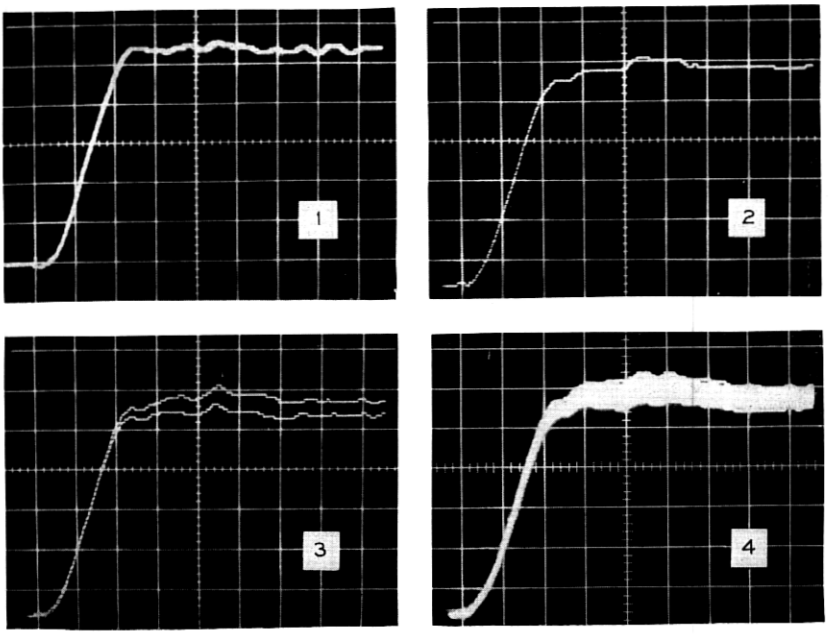


Fig. 13—Table displacement as a function of time. In the above figures, the table displacement was obtained with a laser interferometer having its digital output converted to an analogue output. The scale of the horizontal axis is 2 ms per division, and the vertical axis is 1.34 $\mu$m per division. Nominally, the table is to step 7 $\mu$m in 7 ms. The very small steps noticeable in the curves are single counts of the laser interferometer representing a displacement of about 0.079 $\mu$m. The first two curves each show a single step. The difference between them shows the effect of variations in friction and axial stiffness along the length of the ball screw. The third figure shows two successive steps. The discrepancy between them represents error introduced by the stepping motor. The fourth curve shows 50 successive steps.

the rotational motion superimposed on the translational motion was less than 10 seconds of arc and that the transverse motion was about one micron.

## V. ACKNOWLEDGMENT

The authors wish to acknowledge J. W. West's contribution to the fundamental ideas involved in the stepping system and decagonal mirror adjustment.